Supplementary Information

Materials and Methods

Patient-Derived Xenografts (PDX) and breast-cancer cell-lines

Four-to-eight-week-old female Rag2$^{-/-}\gamma_c^{-/-}$ mice were used to generate breast cancer PDX following guidelines for treatment of laboratory animals of United States National Institutes of Health (NIH). The UC San Diego Medical Experimental Animal Care Committee approved the study protocol. The mice were housed in laminar-flow cabinets under specific pathogen-free conditions and fed *ad libitum*. We enzymatically/mechanically dissociated breast cancer biopsy material into single cells and implanted washed, viable cells into Rag2$^{-/-}\gamma_c^{-/-}$ mice. Early passage (P1-P5) of primary tumor tissues from these PDX models were dissociated enzymatically/mechanically using *GentleMACS Dissociator* (Miltenyi Biotec), as per the manufacturer's guidelines. Erythrocytes were removed via density gradient centrifugation in Percoll Plus (GE Healthcare Life Sciences, CC-17-5442-01).

Hs578T cells were obtained from the American Type Culture Collection (ATCC, Manassas, VA) in 2017. The identity of each cell line was confirmed by short tandem repeat profiling of 10 loci using the GenePrint 10 system (Promega). *Mycoplasma* testing of cell cultures was carried out routinely using the MycoAlert Mycoplasma Detection Kit (Lonza), most recently in May 2018. Cells were passaged no more than 18 times before a low-passage batch was thawed. Cells were growing in DMEM containing 10% FBS and 10 µg/mL insulin.

Tumorigenicity assay

Cells were suspended in Mammary-Epithelial Growth Medium (MEGM), mixed with Matrigel (BD Biosciences, San Diego, CA) at a 1:1 ratio, and then transplanted into the mammary pads of $Rag2^{-/-}\gamma_c^{-/-}$ mice. We monitored the mice weekly for the development of tumors. We extirpated tumors to examine the breast cancer cells for expression of ROR1 at 10 days after treatment with 13.4 mg/kg paclitaxel delivered via intravenous injection on each of consecutive 5 days.

To examine for metastases, we harvested the lungs of 6 mice from each treatment group at 42- or 48-days after engraftment and fixed the tissue with 10%-formalin, prior to paraffin embedding. Each paraffin block was cut into 200-μm sections. Tumor foci were scored in a blinded fashion by a board-certified pathologist.

To test whether cirmtuzumab alone or in combination with paclitaxel affected the growth of primary breast tumor cells, $1x10^5$ single cells isolated from PDX4 or PDX5 were injected into the mammary pads of 4- to 6-week-old $Rag2^{-/-}\gamma_c^{-/-}$ mice. When the mice developed tumors of 300 mm^3 in size, they received paclitaxel at 13.4 mg/kg intravenously on each of 5 consecutive days and/or cirmtuzumab at 10 mg/kg intravenously twice, spaced 1 week apart, and then biweekly thereafter. Control groups were similarly treated instead with hIgG or irrelevant specificity. The tumor volume (v) was determined using the formula $v = (\text{length}) \times (\text{width})^2 \times 0.4$. Mice were monitored for 6- or 8-weeks after the implantation of tumor cells for tumor engraftment using an extreme limiting dilution assay.

RNA-Seq sample preparation and sequencing

Total RNA was prepared from tumor tissues excised using the Trizol RNA-extraction protocol with subsequent purification of RNA using RNeasy columns (Qiagen kit). Total RNA was assessed for quality using an Agilent Tapestation. Samples had RNA Integrity Numbers (RIN) ranging from 9.2 to 9.9. RNA libraries were generated from 1 μg of RNA using Illumina's TruSeq Stranded mRNA Sample Prep Kit, following the manufacturer's instructions, modifying the shear time to 5 minutes. RNA libraries were multiplexed and sequenced with 50 base pair (bp) single end reads (SR50) to a depth of approximately 40 million reads per sample on an Illumina HiSeq4000.

We applied standard RNA-seq analytical pipeline to the eight samples. Briefly, adapters were removed and reads were trimmed of bases with low quality scores in late sequencing cycles using Cutadapt, which removes adapter sequences from high-throughput sequencing reads (1). We then mapped the reads to human genome build 38, using the STAR aligner (v2.5.2b) (2). RSEM (v1.3.0) (3) was used to obtain the raw gene counts from the read alignments and Ensemble gene models (v83) (4). We used package DEseq2 (5) to normalize the read count data and Illumina software package to assess for differential expression. The data were deposited in a GEO database (GSE108632).

Gene set enrichment analyses

We used the GSEA software (6) for gene-set-enrichment analyses (GSEA) on the primary microarray data available in the GEO database under accession numbers GSE87455 (7) and GSE21974 (8). We also performed GSEA on RNA-Seq data (GSE108632) generated from PDX isolated mice treated with cirmtuzumab or control human IgG (hIgG). Microarray data, obtained from 50 breast cancer samples collected before (n=25) and

after (n=25) chemotherapy (Tx) (GSE21974) or from 122 breast cancer samples from GSE87455 dataset, were ranked by their relative expression of ROR1. Of these cases, tumors with a ROR1 expression value above the median for all samples were designated as $ROR1^{Hi}$, whereas tumors with ROR1 expression value below the median value were designated as $ROR1^{Low}$. We ranked genes by their association with the breast cancer groups ($ROR1^{Hi}$ versus $ROR1^{Low}$) using a GSEA signal-to-noise ratio ranking metric. We focused GSEA on 3 pathways: Rac1 in BIOCARTA database, cdc42 in Pathway Interaction Database (9, 10), and RhoA in Ingenuity Pathway database (IPA ®,QIAGEN Redwood City, www.qiagen.com/ingenuity). Each gene set was considered significant when the false discovery rate (FDR) was less than 25% (6). For each gene set tested, we determined the gene-set size (SIZE), the enrichment score (ES), the normalized ES (NES), the nominal p value (NOM p-val), and the FDR q value (FDR q-val). The FDR q value was adjusted for gene set size and multiple hypothesis testing.

Flow cytometry analysis

Single-cell suspensions were treated with Fc-blocking (Miltenyi Biotec), and then stained with Fluorescein-conjugated anti-CD44 (#555479), phycoerythrin (PE)-conjugated anti-CD24 (#561646, Pharmingen), Alexa-647-conjugated 4A5 (11), PE-conjugated anti-EpCAM (#347198, BD Biosciences), and phycoerythrin (PE)-conjugated anti-HLA-A2 (#343306, Biolegend). ALDH1 activity was detected according to method described previously (12). Data were acquired using a FACS-Calibur or FACS-Aria (Becton Dickinson) and were analyzed using the FlowJo software (Tree Star). Forward light scatter (FSC) and side-light scatter (SSC) gating was used to exclude cell debris. Furthermore, we excluded cells that stained with propidium iodide (PI, Sigma) and gated

on cells that stained with Calcein Violet (Life Technology) for viable cell analysis. Finally, gating on cells that bound to a mAb specific for human EpCAM allowed us to examine for breast cancer epithelial cells.

Cell-Invasion assay

$5x10^4$ viable single cells from primary tumors were suspended in MEBM growth medium (Lonza, MD), plated in invasion chambers (8-μm pore size, BD Biosciences), and cultured with or without cirmtuzumab (50 μg/ml) overnight. The lower chambers were filled with serum-free, conditioned medium collected from NIH3T3 cells. Invasion assay for cell lines were performed as described (13). The cells on the apical side of each insert were scrapped off. Invasive cells were fixed with 4% paraformaldehyde and stained by Diff-Quick staining kits (IMEB Inc, San Marcos, CA) and visualized with an inverted microscope (Nikon). A more detailed description of the reagents, biochemistry assays, cellular analysis and animal studies are provided in SI Appendix, Materials and Methods.

Immunohistochemistry staining

For immunohistochemistry staining, primary tumors or lung organs excised from mouse xenografts were fixed in formalin. Lung tissue sections were prepared and stained with Hematoxylin & Eosin (H&E), Hematoxylin, or anti-ROR1 antibody (4A5) as described previously (14). Images were collected using a Delta Vision microscope. The levels of ROR1 were scored on the following scale as described (14); A score of 0 indicated that none of the cancer cells in the sample stained with the anti-ROR1 mAb; a score of 1 indicated low-level binding of the mAb to the tumor cells or low-to-moderate-level binding of the mAb to less than 50% of tumor cells; a score of 2 indicates moderate-level staining on more than 50% of tumor cells or high-level staining of the tumor cells on less than 50%

of tumor cells; a score of 3 indicates high-level staining of the tumor cells on more than 50% of tumor cells. All staining was evaluated by a board-certificated pathologist.

Immunofluorescence staining

Cells were cultured on coverslips to appropriate density or spun onto slides using a cytocentrifuge. Cells were fixed with 4% paraformaldehyde and permeabilized with 0.1% Triton X-100 in PBS. After the cells were washed twice with PBS, they were blocked with 1% BSA in PBS for 30 minutes. Control antibodies or rabbit anti-YAP/TAZ (#8418, Cell Signaling Technology) or mouse 4A5 was added in blocking buffer and incubated for 1.5 hours. After washing the cells with PBS, they were incubated with Alexa Fluor 594-conjugated anti-rabbit secondary antibodies or Alexa Fluor 488-conjugated anti-mouse secondary antibodies for 1.5 hours. The cells were washed again and mounted onto slides using ProLong Gold Antifade Reagent with DAPI (Life Technologies). The images were obtained and analyzed by using an Olympus FV1000 confocal microscope. The percentage of the nuclear localized YAP/TAZ was analyzed by Intensity measurement of Image J software. Nuclear localized YAP/TAZ was calculated by subtracting the YAP/TAZ signal intensity for the cytosol from the YAP/TAZ signal intensity for the total cell. The percentage of nuclear YAP/TAZ was calculated by dividing the nuclear-localized YAP/TAZ signal by YAP/TAZ signal for the entire cell.

CRISPR/Cas9 genome editing

SpCas9 and chimeric guide RNA expression plasmid PX330 (Addgene) were used to generate stable ROR1 knockout cell lines as described (16). CRISPR targeting sequence (CCAGTGCGTGGCAACAAACGGCA) of ROR1 were designed with CRISPR Design tool (http://crispr.mit.edu/). Hs578T transfected with ROR1 CRISPR plasmids were stained for

ROR1 using 4A5-Alex647 and the ROR1-negative cells isolated and placed into culture. This process was repeated 3 successive times to isolate a population of ROR1 knock-out cells.

Immunoblot analyses

Cells used for examination of proteins via immunoblot analysis were treated with control antibody or cirmtuzumab (50 μg/ml) for overnight and then were cultured in medium supplemented with or without recombinant Wnt5a (100 ng/ml). Treated cells or tissues were lysed in buffer containing 1% NP40, 0.1% SDS, 0.5% sodium deoxylate, and protease inhibitors (Pierce). Size-separated proteins were transferred to membranes, which were incubated with primary antibodies specific for ROR1 (#4102), TAZ (#4883), YAP (#14074), pAKT(#4060S), AKT (#4691S), β-Actin (#3700, Cell Signaling Technology), BMI1 (#ab135713, Abcam), Rac1 (#ARC03), RhoA (#ARH04), cdc42 (#ACD03, Cytoskeleton), or Wnt5a (#MAB645, R&D system). After washing away unbound antibody, the membranes were incubated with secondary antibodies that were conjugated with horseradish peroxidase. Blots were prepared for enhanced chemiluminescence and autoradiography. The protein concentration was determined using a bicinchoninic acid protein assay (Pierce).

Assays for activated Rho-GTPases

RhoA and Rac1 activation assay reagents were purchased from Cytoskeleton and used according to the manufacturer's instructions. Briefly, GTP-bound active RhoA, Rac1 or cdc42 was pulled down with Rhotekin-RBD or PAK-PBD beads, respectively, and then examined via immunoblot analysis. Immunoblots of whole-cell lysates were used to assess for total RhoA, Rac1, or cdc42. The integrated optical density (IOD) of each band

was evaluated by densitometry and analyzed using Gel-Pro Analyzer 4.0 software (Media Cybernetics).

Quantitative PCR

Total RNA was extracted using Trizol (Life Technologies). A 10-μg volume of total RNA was incubated with 10 U RNase-free DNase I (Life Technologies) at 37°C for 30 minutes. RNA was purified using RNeasy (QIAGEN). The purified total RNA (2 μg) was converted to cDNA using 200 U Superscript III Reverse Transcriptase (Life Technologies). Taq 2x Master Mix (NEB) was used for PCR according to the manufacturer's protocol.

Silencing of human AKT

AKT siRNA was purchased from Cell Signaling. All siRNA transfections were performed in DMEM serum-free medium using lipofectamine RNAiMAX (Invitrogen), according to the manufacturer's instructions, and then subjected to different assays.

Statistical analyses

Unless indicated otherwise, data were presented as the mean ± standard error of the mean (SEM). Differences between two groups were determined by unpaired 2-tailed Student's t-Test. Differences between multiple groups were determined by Dunnett's multiple comparison test. All P values of less than 0.05 were considered significant. Analysis for significance was performed with GraphPad Prism 6.0 (GraphPad Software Inc.).

Sequence of primers for qPCR

GAPDH primers:	5’-GAAGGTGAAGGTCGGAGTC-3’ (forward)
	5’-GAAGATGGTGATGGGATTTC-3’ (reverse)
BMI1 primers:	5’-CGTGTATTGTTCGTTACCTGGA-3’ (forward)
	5’-TTCAGTAGTGGTCTGGTCTTGT-3’ (reverse)

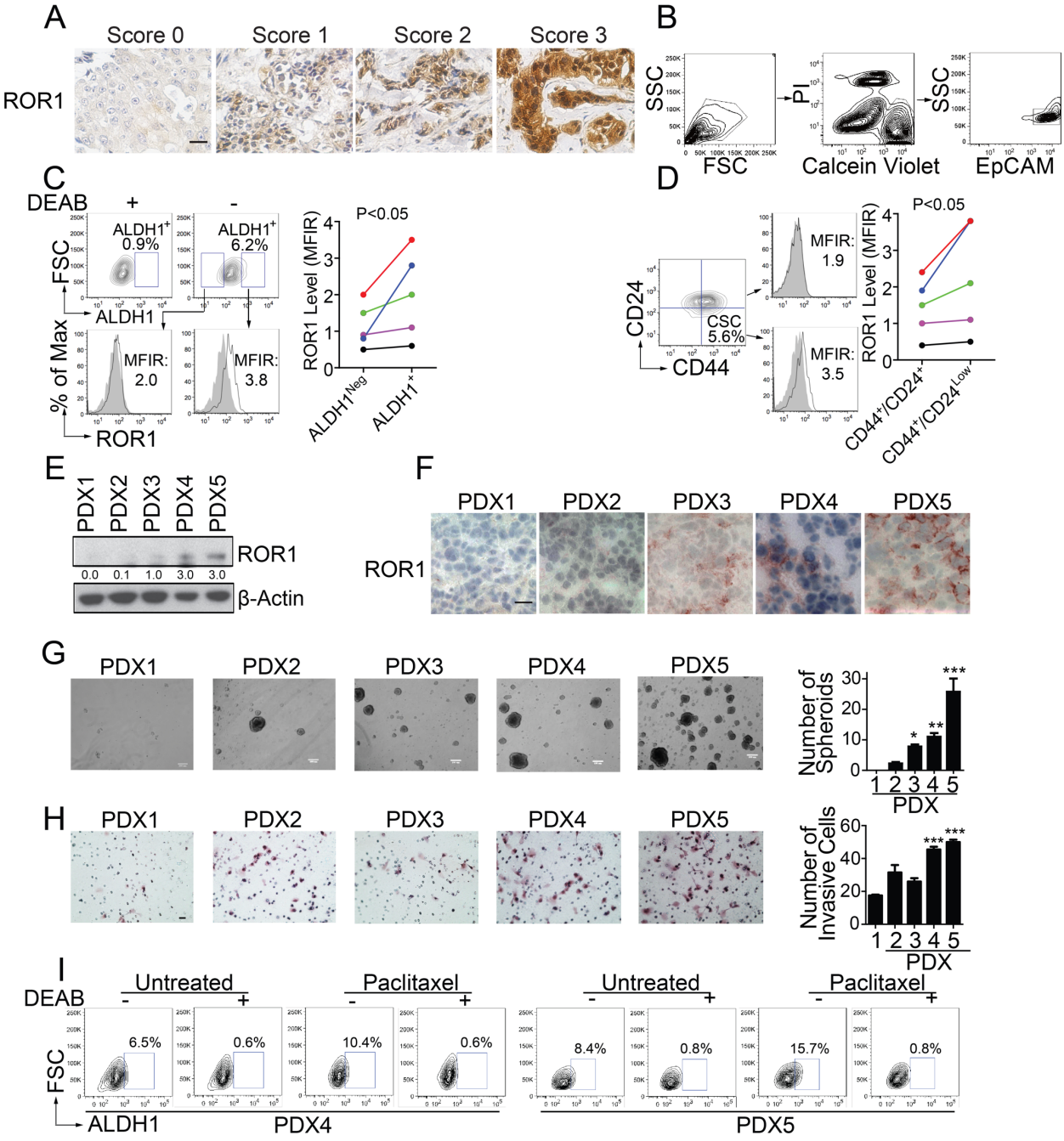

Fig. S1. ROR1^{Hi} Breast Cancers Have Enhanced Stemness Features

(*A*) Representative images of breast cancer tissues stained with the anti-ROR1 mAb, 4A5. The bound antibody is brown and the nuclear counterstain with hematoxylin is blue.

Scale bar: 25 μM. (*B*) Gating strategy for primary tumor cells isolated from each PDX. Single-cell suspensions were made from extirpated tumor nodules and stained with propidium iodide (PI), Calcein Violet or fluorescein diacetate (FDA), and fluorochrome-conjugated mAb specific for EpCAM, or an irrelevant antigen (control). We gated on cells having the appropriate forward light scatter (FSC) and side scatter (SSC) characteristics (left). We excluded dead cells labeled with PI and gated on live cells that stained with Calecein Violet (middle). Because the cells also were stained with fluorochrome-conjugated mAbs, we gated on human breast cancer cells that were stained with mAbs specific for EpCAM (right). (*C*) Cells from each PDX were stained for ROR1 with 4A5 or control mAb, and for ALDOFLUOR without (-) or with (+) the ALDH1-inhibitor, DEAB, as indicated at the top of each column of histograms. The open boxes in each contour plot in the top row indicate the gates used for defining cells with ALDH1 activity, the proportions of which are indicated. The open boxes in the left of the contour plots depict the gates used to identify cells that assuredly lacked ALDH1 activity. In the bottom row are histograms depicting the fluorescence of cells that were negative (left) or positive (right) for ALDH1 activity. The right panel provides the staining intensity for ROR1 in $ALDH1^{+}$ versus $ALDH1^{Neg}$ cells from each of the five different PDX tumors. (*D*) Cells from each PDX were stained with CD44, CD24, 4A5, or a control mAb. The histograms depict the fluorescence of gated $CD44^{+}/CD24^{Low}$ or $CD44^{+}/CD24^{+}$ cells; the shaded histograms depict the fluorescence of cells stained with an isotype-control mAb, whereas the open histograms depict the fluorescence of cells stained with 4A5. The right panel provides the ROR1 staining intensity of $CD44^{+}/CD24^{Low}$ versus $CD44^{+}/CD24^{+}$ cells from each of five different PDX. The number in each plot provides the mean fluorescence intensity ratio

(MFIR) for ROR1, which is derived from the mean fluorescence intensity (MFI) of cells labeled with the anti-ROR1 mAb divided by MFI of cells labeled with control antibody. (*E*) Lysates from each of PDX were examined for ROR1 expression via immunoblot analysis. β-Actin serves as loading control. (*F*) Tissue sections of PDX1-5 were stained with 4A5 for detection of ROR1 by IHC. Staining for bound 4A5 is in red and staining for nuclear material is in blue. Scale bar: 15 μm. (*G*) Photomicrographs of spheroids generated by cells isolated from each of PDX. Scale bar: 100 μm. The bar graph depicts the average numbers of spheroids formed by cells from each PDX in triplicate wells ± SEM. (*H*) Representative photomicrographs of invasive cells from isolated tumor cells of each PDX. To the right of the photomicrographs are bar graphs depicting the mean relative proportions of tumor cells that migrated into Matrigel (±SEM) from each tumor cell population in three independent experiments, each normalized to the proportion of the tumor cells from PDX5 that migrated into Matrigel. Scale bar: 10 μm. An asterisk represents $P < 0.05$, ** denotes $P < 0.01$, and *** represents $P < 0.001$, using Dunnett's multiple comparison test. (*I*) Single cell suspensions were generated from each PDX that were removed from PDX-engrafted mice that had not received treatment (Untreated), or had been treated with paclitaxel. We examined for ALDH1 enzymatic activity via flow cytometry. DEAB, an inhibitor of ALDH1 enzymatic activity, was used to identify cells that have ALDH1 activity. The open boxes in the right of the contour plots depict the gates used to identify cells that are certain to have ALDH1 activity. The number in each histogram depicts percentage of $ALDH1^+$ cells.

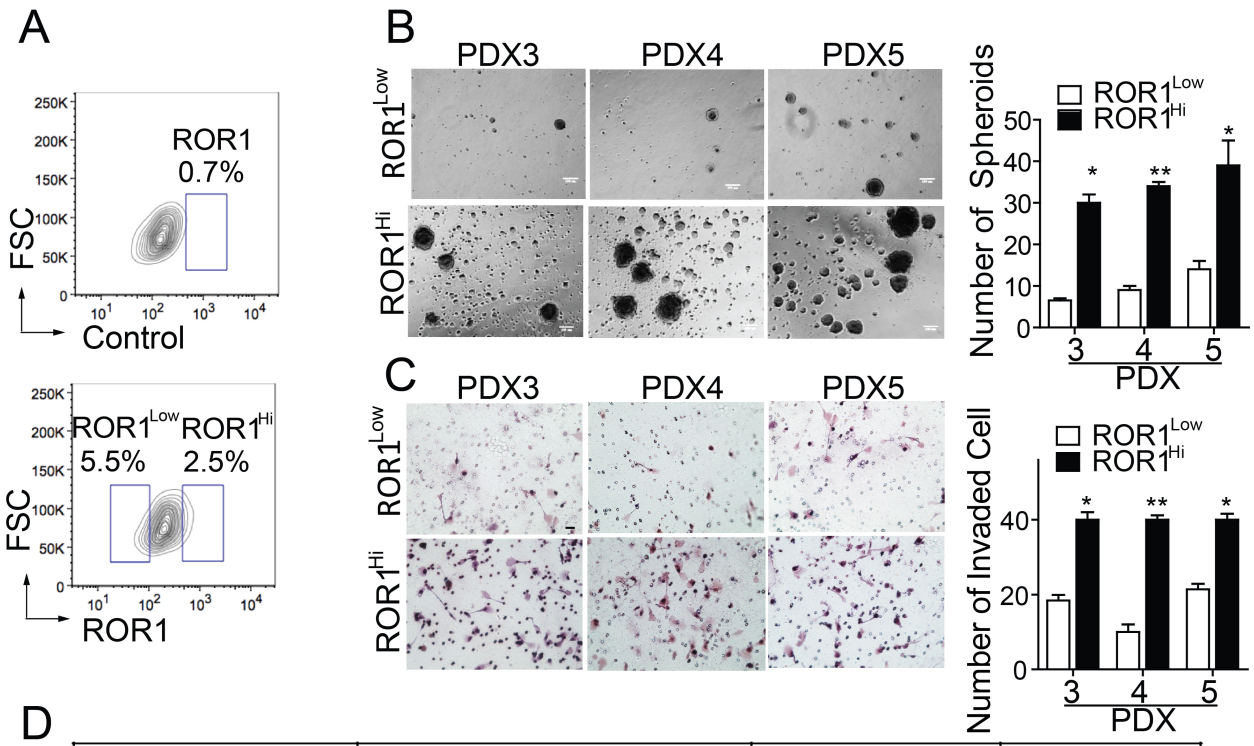

Tissue ID		Cell Number			Frequency of Tumorigenic Cell	P Value
		5000	500	100		
PDX3	$ROR1^{Low}$	0/4	0/9	0/10	1/2913	<0.01
	$ROR1^{Hi}$	2/5	5/10	1/10	Inf	
PDX4	$ROR1^{Low}$	3/6	2/6	N.D	1/455	<0.001
	$ROR1^{Hi}$	6/6	4/6	N.D	1/4740	
PDX5	$ROR1^{Low}$	N.D	1/9	0/10	1/329	<0.001
	$ROR1^{Hi}$	N.D	8/9	1/10	1/5247	

Fig. S2. $ROR1^{Hi}$ Breast Cancer Cells Have Stemness Features

(*A*) Strategy for sorting $ROR1^{Hi}$ versus $ROR1^{Low}$ cells. The open boxes indicate the gates used to select $ROR1^{Low}$ (left) or $ROR1^{Hi}$ (right) cells. (*B*) Photomicrographs of spheroids formed from $ROR1^{HI}$ or $ROR1^{Neg}$ cells isolated from each of the PDX, as indicated on the top. Scale bar: 100 μm. The bar graph to the right depicts the average numbers of spheroids formed ± SEM by each of the cell preparations in three separate cultures, as indicated at the bottom of the histograms. (*C*) Photomicrographs of Matrigel-invading cells

from ROR1^{HI} or ROR1^{Low} cells isolated from different PDX, as indicated on the top. Scale bar: 10 μm. The bar graph to the right depicts the mean invaded cells into Matrigel (±SEM) per field for 10-20 fields of each of the cell preparations in three independent experiments. (*D*) Tumor incidence in animals implanted with ROR1^{Hi} or ROR1^{Low} cells isolated from each of the various breast cancer PDX. Frequency of tumorigenic cells and probability estimates were computed using ELDA software. N.D indicates not done.

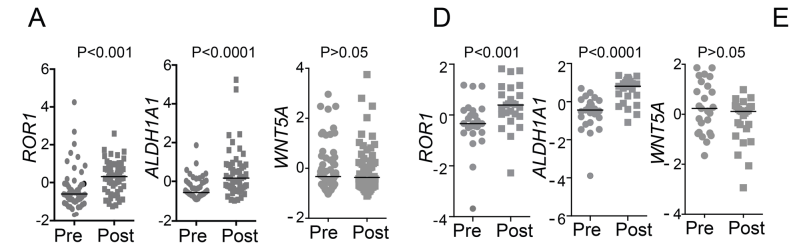

E

Gene Sets	Size	ES		NES		NOM p-val		FDR q-val	
		ROR1^{Hi} vs *ROR1*^{Low}	Post vs Pre	*ROR1*^{Hi} vs *ROR1*^{Low}	Post vs Pre	*ROR1*^{Hi} vs *ROR1*^{Low}	Post vs Pre	*ROR1*^{Hi} vs *ROR1*^{Low}	Post vs Pre
CD44^{+}/CD24^{Low} MS	99	0.46	0.52	1.61	2.16	0.03	0.00	0.07	0.00
EMT	220	0.52	0.31	1.78	1.47	0.00	0.00	0.00	0.03
Rac1 Pathway	22	0.48	0.52	1.44	1.61	0.05	0.01	0.08	0.01
RhoA Pathway	45	0.44	0.41	1.34	1.52	0.12	0.03	0.12	0.02
cdc42	30	0.46	0.35	1.47	1.19	0.05	0.22	0.12	0.16
Hippo-Yap	57	0.53	0.36	1.60	1.33	0.04	0.07	0.03	0.07
BMI1	143	0.32	0.42	1.17	1.90	0.20	0.00	0.20	0.00

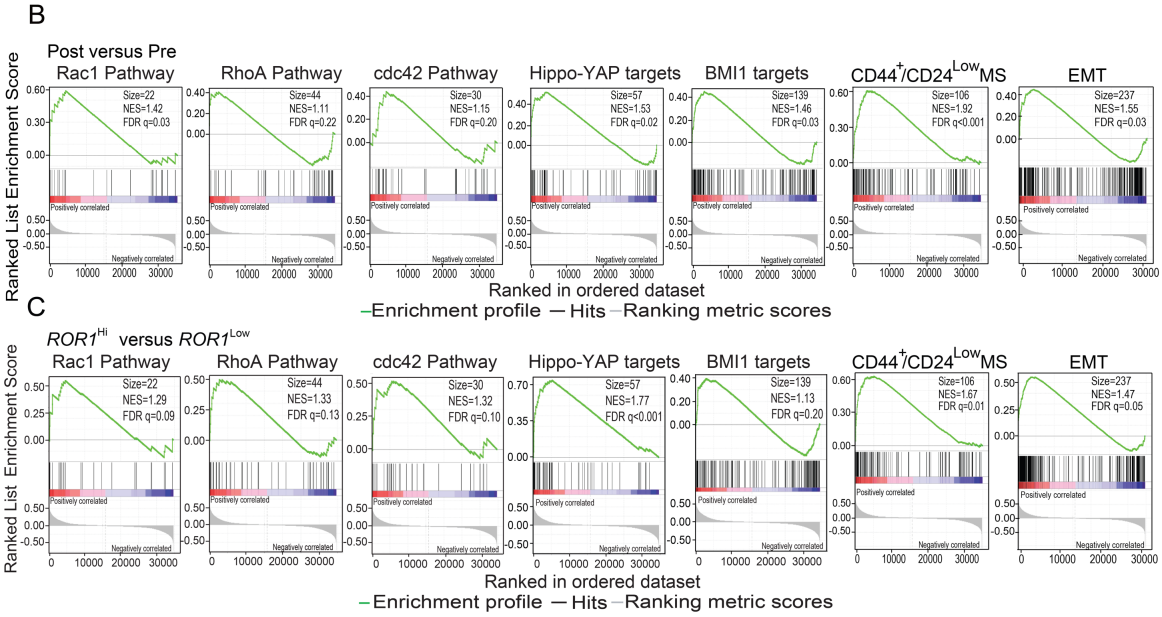

Fig. S3. Chemotherapy Can Enhance Breast Cancer Expression Of ROR1, Genes Associated With Breast Cancer Stemness

(*A*) *ROR1*, *ALDH1A1*, *Wnt5a* expression levels in matched breast cancer patient samples before ("Pre") or after chemotherapy ("Post") (Post, Pre, N=57, GSE87455). (*B*) Enrichment plots of genes activated by Rac1/RhoA/cdc42-signaling, Hippo-YAP target genes, BMI1 target genes, gene signature of CD44^{+}/CD24^{Low} MS population and of gene associated with EMT on post-treatment samples (N=57) versus matched pre-treatment samples (N=57) in the GSE87455 dataset. The middle portion of the plot shows where the members of the gene set appear in the list of ranked genes; red and blue colors represent positive and negative correlation with the level of *ROR1* expression,

respectively. (*C*) Enrichment plots of genes activated by Rac1/RhoA/cdc42-signaling, Hippo-YAP target genes, BMI1 target genes, gene signature of $CD44^{+}/CD24^{Low}$ MS population and of genes associated with EMT for the *ROR1*^{Low} and *ROR1*^{Hi} sample groups from the GSE87455 (N=122). The middle portion of the plot shows where the members of the gene set appear in the list of ranked genes; red and blue colors represent positive and negative correlation with the level of *ROR1* expression, respectively. (*D*) *ROR1, ALDH1A1* or *Wnt5a* expression levels in matched breast cancer patient samples before ("Pre") or after chemotherapy ("Post") (Post, Pre, N=25, GSE21974). The line indicates the median expression level of genes in pre- versus post-treatment group. (*E*) Gene Set Enrichment (GSE) Analysis for genes associated with $CD44^{+}/CD24^{Low}$ MS, ETM, activation of Rac1/RhoA/cdc42, Hippo-YAP, BMI1 for the *ROR1*^{Low} and *ROR1*^{Hi} sample groups (N=25) or on breast cancer biopsies from patients who received neoadjuvant chemotherapy (N=25) Versus Matched Pre-treatment Samples (N=25) in the GSE21974 database. SIZE is the number of genes included in the analysis. NES (normalized enrichment score) accounts for the difference in gene-set size and can be used to compare the analysis results across gene sets. NOM p-val (nominal p value) is the statistical significance of the enrichment score not adjusted for gene set size or multiple gene sets testing, FDR q-val (false discovery rate q value) is the estimated probability that a gene set with a given NES represents a false positive. Each gene set is considered significant when the false discovery rate (FDR) is less than 0.25.

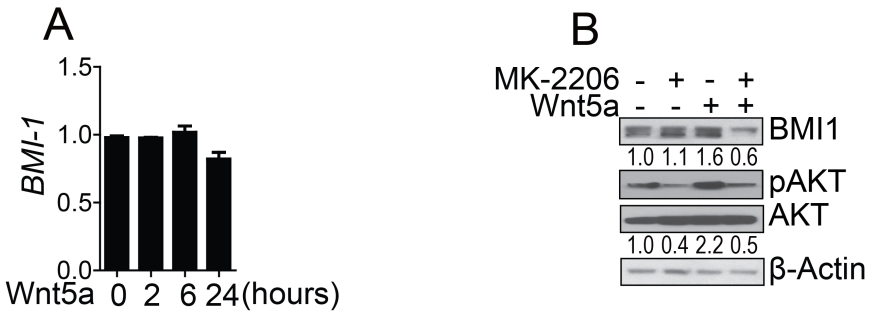

Fig. S4. Wnt5a Can Enhance Breast Cancer Expression BMI1 Protein

(*A*) *BMI1* mRNA level in Hs578T cells treated with Wnt5a at 100ng/ml at indicated time point were examined by quantitative PCR (qPCR). Data shown were the mean expression levels of *BMI1* relative to time 0 samples in triplicate and normalized with respect to GAPDH. Error bars indicate SEM. (*B*) Hs578T cells were cultured in serum-free medium, pre-treated with or without MK-2206 for 3 hours, and then stimulated with or without Wnt5a at 100ng/ml for 6 hours. BMI1, pAKT and AKT were examined on these samples via immunoblot analyses. Numbers below the row for AKT provide the ratios of band densities of pAKT to AKT that were normalized to that of samples treated for 0 minutes with Wnt5a. β-Actin served as protein-loading control. Numbers below the row for BMI1 provide the ratios of band densities of BMI1 to β-Actin, normalized with respect to that of samples treated for 0 minutes with Wnt5a.

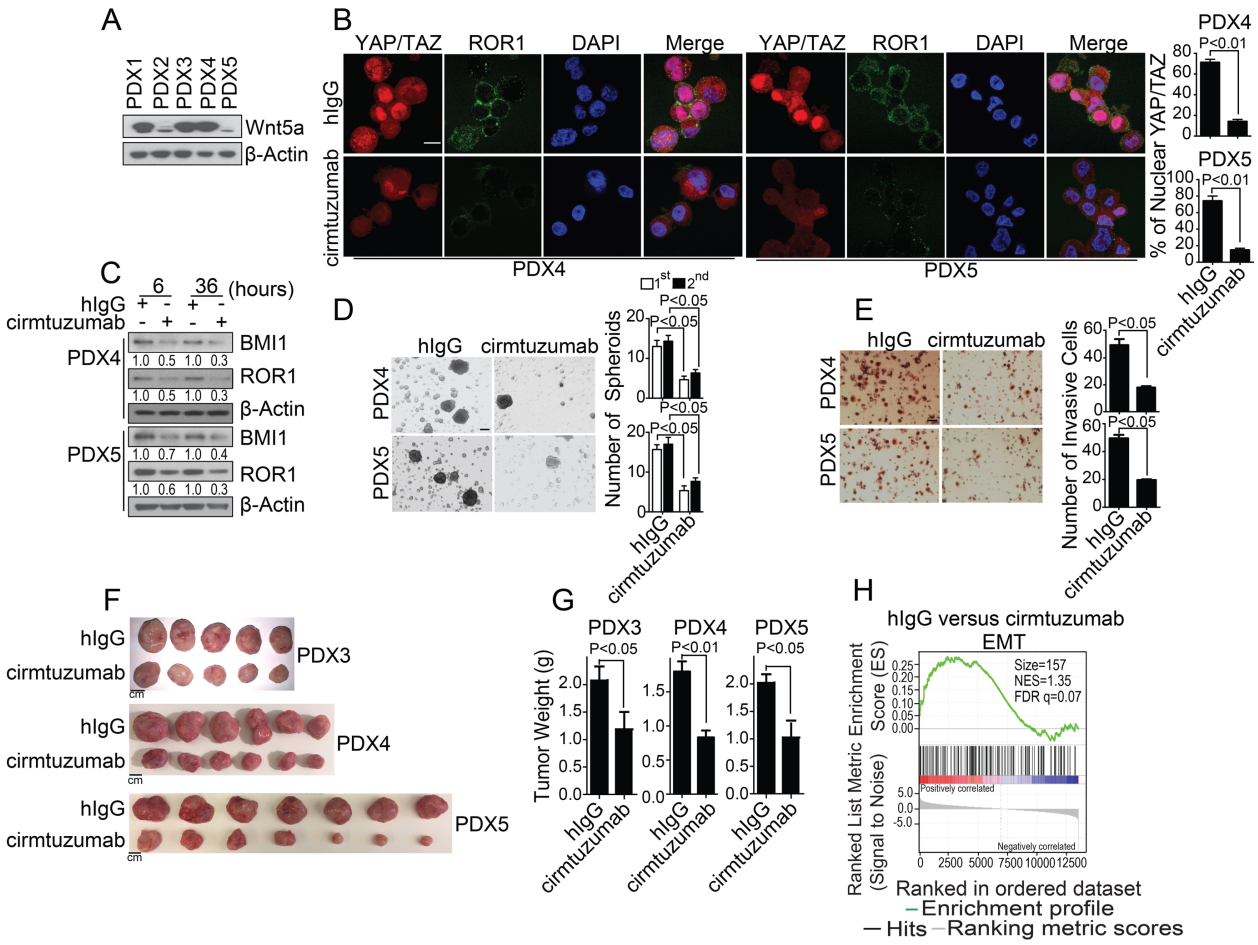

Fig. S5. Treatment With Cirmtuzumab Could Inhibit YAP/TAZ Activity And BMI1 Expression In Vitro And Repress Tumor Growth In Vivo

(*A*) Lysates from PDX1-PDX5 were examined for expression of Wnt5a, as indicated on the right margin. β-Actin serves as loading control. (*B*) Single cell suspension isolated from PDX4 or PDX5 treated with cirmtuzumab antibody or control antibody at 50 μg/ml for 4 hours were examined for YAP/TAZ via confocal microscopy. Right bar graph provides the average percentages of nuclear YAP/TAZ in the cells of each field. Scale bar: 20 μm. (*C*) Lysates from PDX4 or PDX5 treated with cirmtuzumab antibody or control antibody at 50 μg/ml for the indicated times were examined for BMI1, ROR1 or β-Actin via immunoblot analyses. (*D*) Representative photomicrographs of spheroids formed from

isolated tumor cells of different PDX treated with either control antibody or cirmtuzumab at 50 µg/ml. The bar graph on right panel depicts the average numbers of spheroids formed from tumor cells of PDX4 or PDX5 treated with cirmtuzmab or a control antibody in three separate culture wells of each treatment ± SEM. (*E*) Representative photomicrographs of invasive cells from isolated tumor cells of different PDX treated with either control antibody or cirmtuzumab at 50 µg/ml. To the right of the photomicrographs are bar graphs depicting the mean number of invaded cells of each of the cell preparations in three independent experiments ± SEM. Scale bar: 10 µm. (*F*) $1X10^6$ cells from each PDX sample in 50 µl were mixed with equal volumes of Matrigel and then injected into the mammary pad of female $Rag2^{-/-}\gamma_c^{-/-}$ mice. Tumor growth was monitored over time for 42 or 48 days. Representative photographs of each PDX removed at 42 (PDX5) or 48 (PDX4) days. Scale bar: 1 cm. (*G*) The bar graph provides average weight of tumors extirpated from the mice in each group described in figure 1A (± SEM, N=5-8). (*H*), Enrichment plots of genes associated with EMT in PDX derived from PDX4 in mice treated with control hIgG versus cirmtuzumab, as assessed via RNAseq (GSE108632).

Table S1
Clinical and Pathologic Characteristics Of Tumors From Patients Who Received Neoadjuvant Therapy

Patient Number	ER/PR/HER2 Status	Treatment	ROR1	
			Pre	Post
1	$ER^-/PR^-/HER2^+$	TEC	1	2
2	$ER^-/PR^-/HER2^-$	TE	2	3
3	$ER^-/PR^-/HER2^+$	TE	3	3
4	$ER^-/PR^-/HER2^+$	TE	1	3
5	N.D	TEC	2	2
6	N.D	TEC	2	2
7	$ER^+/PR^-/HER2^-$	TEC	2	2
8	$ER^-/PR^-/HER2^-$	TE	2	3
9	$ER^+/PR^+/HER2^-$	TAC	1	3
10	$ER^-/PR^-/HER2^-$	TE	2	3
11	$ER^+/PR^-/HER2^-$	TE	1	2
12	$ER^+/PR^+/HER2^-$	TEC	2	2
13	$ER^+/PR^+/HER2^-$	TE	2	3
14	$ER^+/PR^-/HER2^+$	TEC	3	3
15	$ER^+/PR^+/HER2^-$	TE	2	3
16	$ER^+/PR^+/HER2^-$	TEC	1	3
17	N.D	TE	1	0
18	$ER^-/PR^+/HER2^-$	TEC	2	3
19	N.D	TEC	2	3
20	$ER^+/PR^+/HER2^-$	EC	2	2
21	$ER^-/PR^-/HER2^+$	TEC	1	2
22	$ER^+/PR^+/HER2^-$	TEC	2	3

N.D: Not Defined

Table S2

Clinical, Pathologic Characteristics And Proportion Of CSCs Markers Expression Of Tumors Used To Generate Each PDX

PDX ID	ER/PR/HER2 status	Histology	P53 mutation status	Prior treatment	Expression of CSCs Markers		
					$ALDH1^+$	$CD44^+$	$CD44^+/CD24^{Low}$
PDX1	$ER^-/PR^-/HER2^+$	Ductal Carcinoma Primary Tumor	N/A	Taxane/ Platinum/ Trastuzumab	0.6%	1.8%	0.1%
PDX2	$ER^-/PR^-/HER2^-$	Ductal Carcinoma Primary Tumor	no mutations	None	2.9%	63.1%	48.8%
PDX3	$ER^-/PR^-/HER2^-$	Mixed Ductal and Lobular Carcinoma Primary Tumor	P53 mutation	Anthracycline / Taxane	3.5%	76.1%	5.6%
PDX4	$ER^-/PR^-/HER2^-$	Ductal Carcinoma Primary Tumor	P53 mutation	Taxane	6.5%	23.9%	2.3%
PDX5	$ER^+/PR^-/HER2^-$	Ductal Carcinoma Axillary Lymph Node	P53 mutation	N/A	8.4%	85.0%	6.2%

Table S3

Tumor Incidence In Animals Implanted With Different Subpopulations Of Cells Isolated From Breast Cancer PDX

Subpopulation	Cell Number		Frequency of Tumorigenic Cell	P Value
	500	100		
$CD44^{+}/CD24^{Low}$	3/4	2/4	1/265	0.002
$CD44^{+}/CD24^{+}$	0/4	0/4	1/Inf	
$ALDH1^{+}$	2/5	1/5	1/800	0.04
$ALDH1^{Neg}$	0/4	0/4	1/Inf	

$CD44^{+}/CD24^{Low}$ versus $CD44^{+}/CD24^{+}$ cells isolated from PDX4 or $ALDH1^{+}$ versus $ALDH1^{Neg}$ cells isolated from PDX5 were implanted into mammary pads of $Rag2^{-/-}\gamma_c^{-/-}$ mice (n=4-5). The numbers of mice with tumors 2 months after engraftment divided by the number of mice injected in each group are shown in the table. Frequency of tumorigenic cells and probability estimates were computed using ELDA software. Inf indicates infinite.

Table S4

Gene Set Enrichment (GSE) Analysis Of 9 Stem-Cell Gene-Expression Signatures (15) On The *ROR1*^{Hi} (N=61) Versus *ROR1*^{Low} (N=61) Samples and The *ROR1*^{Low} (N=61) Versus *ROR1*^{Hi} (N=61) Samples From Breast Cancer Patients Prior To Chemotherapy in GSE87455 Database

Gene Sets	Size	ES	NES	NOM p-val	FDR q-val
		ROR1^{Hi} vs *ROR1*^{Low}	*ROR1*^{Hi} vs *ROR1*^{Low}	*ROR1*^{Hi} vs *ROR1*^{Low}	*ROR1*^{Hi} vs *ROR1*^{Low}
Es exp1	359	0.31	0.82	0.72	0.85
Es exp2	35	-0.27	-0.71	0.87	0.97
Nanog targets*	913	0.31	1.01	0.41	0.43
Oct4 targets*	274	0.37	1.19	0.05	0.22
Sox2 targets*	678	-0.33	-1.05	0.25	0.41
NOS targets*	168	0.43	1.34	0.01	0.13
NOS TFs	37	0.55	1.40	0.06	0.10
Myc targets1	227	0.34	1.03	0.38	0.43
Myc targets2	755	-0.42	-1.28	0.04	0.14

An asterisk (*) indicates that the gene set include *ROR1.*

References

1. Martin M (2011) Cutadapt removes adapter sequences from high-throughput sequencing reads. *2011* 17(1):3.
2. Dobin A*, et al.* (2013) STAR: ultrafast universal RNA-seq aligner. *Bioinformatics* 29(1):15-21.
3. Li B & Dewey CN (2011) RSEM: accurate transcript quantification from RNA-Seq data with or without a reference genome. *BMC Bioinformatics* 12:323.
4. Yates A*, et al.* (2016) Ensembl 2016. *Nucleic Acids Res* 44(D1):D710-716.
5. Love MI, Huber W, & Anders S (2014) Moderated estimation of fold change and dispersion for RNA-seq data with DESeq2. *Genome Biol* 15(12):550.
6. Subramanian A*, et al.* (2005) Gene set enrichment analysis: a knowledge-based approach for interpreting genome-wide expression profiles. *Proc Natl Acad Sci USA* 102(43):15545-15550.
7. Kimbung S*, et al.* (2018) Assessment of early response biomarkers in relation to long-term survival in patients with HER2-negative breast cancer receiving neoadjuvant chemotherapy plus bevacizumab: Results from the Phase II PROMIX trial. *Int J Cancer* 142(3):618-628.
8. Stickeler E*, et al.* (2011) Basal-like molecular subtype and HER4 up-regulation and response to neoadjuvant chemotherapy in breast cancer. *Oncol Rep* 26(4):1037-1045.
9. Schaefer CF*, et al.* (2009) PID: the Pathway Interaction Database. *Nucleic Acids Res* 37(Database issue):D674-679.
10. Liberzon A*, et al.* (2011) Molecular signatures database (MSigDB) 3.0. *Bioinformatics* 27(12):1739-1740.
11. Fukuda T*, et al.* (2008) Antisera induced by infusions of autologous Ad-CD154-leukemia B cells identify ROR1 as an oncofetal antigen and receptor for Wnt5a. *Proc Natl Acad Sci U S A* 105(8):3047-3052.
12. Zhang S*, et al.* (2014) Ovarian cancer stem cells express ROR1, which can be targeted for anti-cancer-stem-cell therapy. *Proc Natl Acad Sci USA* 111(48):17266-17271.
13. Cui B*, et al.* (2013) Targeting ROR1 inhibits epithelial-mesenchymal transition and metastasis. *Cancer Res* 73(12):3649-3660.
14. Zhang S*, et al.* (2012) ROR1 is expressed in human breast cancer and associated with enhanced tumor-cell growth. *PLoS One* 7(3):e31127.

15. Ben-Porath I*, et al.* (2008) An embryonic stem cell-like gene expression signature in poorly differentiated aggressive human tumors. *Nat Genet* 40(5):499-507.